ARTICLE

Phosphorene-Based van der Waals Heterojunction for Solar Water Splitting

Peng Wang[a], Jie Meng[a], Jing Huang[b*], Jia-jun Wang[c], Qun-xiang Li[a,d*]

a. Department of Chemical Physics, University of Science and Technology of China, Hefei 230026, China
b. School of Materials and Chemical Engineering, Anhui Jianzhu University, Hefei 230601, China
c. College of Chemistry, Tianjin Normal University, Tianjin 300387, China
d. Hefei National Laboratory for Physical Sciences at the Microscale, University of Science and Technology of China, Hefei 230026, China

(Dated: Received on November 6, 2018; Accepted on November 24, 2018)

As a clean and renewable future energy source, hydrogen fuel can be produced via solar water splitting. Two-dimensional (2D) black phosphorene (black-P) can harvest visible light due to the desirable band gap, which promises it as a metal-free photocatalyst. However, black-P can be only used to produce hydrogen since the oxidation potential of water locates lower than the position of the valence band maximum. To improve the photocatalytic performance of black-P, here, using black-P and blue phosphorene (blue-P) monolayers, we propose a 2D van der Waals (vdW) heterojunction. Theoretical results, including the band structures, density of states, Bader charge population, charge density difference, and optical absorption spectra, clearly reveal that the visible light absorption ability is obviously improved, and the band edge alignment of the proposed vdW heterojunction displays a typical type-II feature to effectively separate the photogenerated carriers. At the same time, the built-in interfacial electric field prevents the electron-hole recombination. These predictions suggest that the examined phosphorene-based vdW heterojunction is an efficient photocatalyst for solar water splitting.

Key words: First-principles, Phosphorene, Band edge alignment, van der Waals heterjunction, Water splitting

I. INTRODUCTION

As a promising technology for conversing solar energy into chemical energy, photocatalytic solar water splitting has attracted extensive attention during the past decades [1−5]. There are two main steps in photocatalytic water splitting [2]: (i) under sunlight radiation, electrons are excited from the valence band (VB) to the conduction band (CB) of a semiconductor photocatalyst, and the electron-hole pairs form; (ii) photogenerated carriers (namely, electrons and holes) have to be effectively separated, and then participate in the hydrogen evolution reaction as well as the oxygen evolution reaction. To ensure the redox reactions can proceed successfully, the redox potentials of photocatalytic water splitting reactions should locate within band gap of photocatalyst. In addition, band gap of photocatalyst is roughly 2.0 eV in order to effectively harvest the visible light [6]. Furthermore, electrons and holes must be spatially separated in order to prevent recombination of them since the recombination of photogenerated carriers will reduce the photocatalytic efficiency. The conventional photocatalysts for solar water splitting, such as TiO_2 [7] and $KTaO_3$ [8], exhibit a low efficiency in utilizing visible light due to their wide band gaps. Other photocatalytic materials, such as SnS_2 [9] and CdS [10], have appropriate band gaps, but the self-oxidation of photogenerated holes has a negative influence on the stability of those photocatalysts. Thus, it is high desirable to design efficient, stable, and environmentally friendly semiconductor photocatalysts for solar water splitting.

Various two-dimensional (2D) materials, such as hexagonal boron nitride monolayers [11, 12], graphitic carbon nitrides (g-C_3N_4 [13], C_2N [14], and g-C_6N_6 [15]), as well as transition metal dichalcogenides [16−18], have recently triggered intensive scientific interest due to their versatile properties for applications in sensors, photodetectors, photocatalysts, *etc.* In addition, the 2D materials provide large surface areas for photocatalytic reaction, and a short migration distance for photogenerated carriers which facilitates their migration to the surface. Among them, recently, black phosphorene (black-P) has been successfully fabricated in experiments via mechanical exfoliation from bulk black phosphorus as a new monoelementary 2D layered material [19−22]. We note that black-P exhibits some

*Authors to whom correspondence should be addressed. E-mail: jhuang@ustc.edu.cn, liqun@ustc.edu.cn

remarkable optoelectronic properties [23], including an direct bandgap of 1.6 eV, a high mobility of hole up to 10^5 $cm^2 \cdot V^{-1} \cdot s^{-1}$ [19], a drain current modulation up to 10^5 [20], and a strong optical absorption of sunlight [24], which are superior to other 2D materials. Therefore, black-P has been considered to be a promising metal-free photocatalyst for solar water splitting [25]. However, the valence band maximum (VBM) and conduction band minimum (CBM) band edge positions of black-P are both more positive than the oxidation potential of O_2/H_2O and the reduction potential of H^+/H_2, respectively. Thus, black-P can only be used as the photocathode for hydrogen evolution reaction in solar water splitting cells [25]. Till now, various techniques, such as electrical bias, mechanical strain, defect, doping, and pH, can be used to tune its band edge positions. For example, Sa *et al.* predicted that strain-engineered black-P can be an effective water splitting photocatalyst at a given pH of 8 based on their first-principles simulations [26]. Hu *et al.* predicted theoretically the enhanced photocatalytic performance of black-P nanoribbons through modifying their edges [27]. Actually, the formation of heterostructures is an effective way for band engineering, which will enhance the separation of photogenerated carriers and then improve the photocatalytic efficiency. So far, several black-P based heterostructures have been proposed experimentally and theoretically as photocatalysts for water splitting, such as black-P/TiO_2 [28, 29] and black-P/MoS_2 [30].

Based on density functional theory calculations, Zhu *et al.* firstly predicted the existence of blue phosphorus (blue-P) [31], which is a new phase of phosphorus, having layered honeycomb structure with high stability. Two years later, Zhang *et al.* obtained monolayer blue-P on Au(111) by means of molecular beam epitaxial growth [32]. The band gap of blue-P on Au(111) is measured to be about 1.10 eV. Theoretical calculations indicated that both VBM and CBM of blue-P are lower than those of black-P monolayer, and the lattice mismatch between the two monolayers is very small. These observations stimulate us to design heterojunction based on black-P and blue-P monolayers since a type-II band edge alignment can be expected.

Here, we explore the photocatalytic performance of the proposed 2D van der Waals (vdW) black-P/blue-P heterojunction by performing extensive hybrid functional first-principles calculations. The calculated band structures, density of states, optical absorption properties, charge density difference, as well as the Bader charge population, clearly reveal that the formation of a type-II vdW heterojunction between the black-P and blue-P monolayers facilitates the effective separation of photogenerated carriers. The built-in interfacial electric field further prevents the recombination of these photogenerated carriers. Moreover, we find that the predicted band structure of the proposed vdW heterojunction is not sensitive to the applied biaxial and vertical strains.

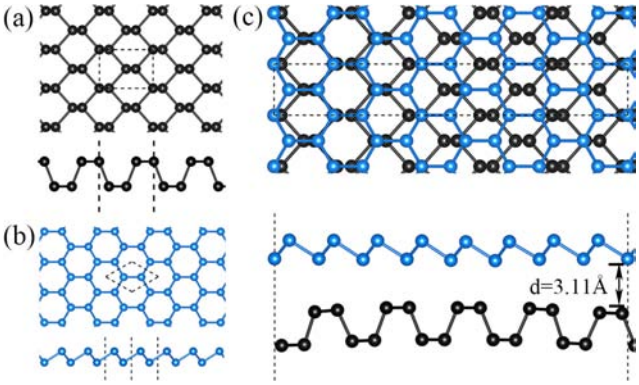

FIG. 1 Top and side views of computational models: (a) black-P monolayer, (b) blue-P monolayer, and (c) the proposed phosphorene-based vdW heterojunction.

These theoretical findings imply that the vdW black-P/blue-P heterojunction is a metal-free photocatalyst with enhanced photocatalytic performance for solar water splitting.

II. COMPUTATION METHODS AND MODELS

In this work, our density functional theory calculations are carried out by using the Vienna *ab initio* simulation package (VASP) [35], which is a projected augmented plane wave method [33, 34]. To accurately describe the weak interaction between the black-P and blue-P monolayers, we adopt the generalized gradient approximation with London dispersion corrections (namely, PBE+D2) [36, 37]. To avoid interaction between neighboring phosphorenes, a vacuum layer of 20.0 Å is used in our calculations. The kinetic energy cutoff for plane-wave basis set is set to be 400 eV, and the Monkhorst-Pack grid to sample the Brillouin zone of the proposed heterojunction is $3\times11\times1$. All atomic positions are fully relaxed with a convergence threshold of 10^{-5} eV in energy and 0.02 eV/Å for the force by using the conjugated gradient method. To obtain accurate electronic structures, we employ the Heyd-Scuseria-Ernzerhof (HSE06) hybrid functional in our calculations [38].

The top and side views of black-P and blue-P monolayers are illustrated in FIG. 1 (a) and (b), respectively, while the proposed phosphorene-based vdW heterojunction is plotted in FIG. 1(c).

III. RESULTS AND DISCUSSION

Before examining the hybrid black-P/blue-P heterojunction, we perform benchmark calculations for the isolated black-P and blue-P monolayers. The optimized lattice constants of black-P are a=4.62 Å, b=3.35 Å, while the lattice constants of the hexagonal blue-P

DOI:10.1063/1674-0068/cjcp1811244

monolayer are a=b=3.31 Å. At the HSE06 hybrid functional levels, the band gap of the free black-P layer is predicted to be 1.51 eV, while for the blue-P layer is about 1.94 eV, according to the calculated band structures. These results are consistent with the previous reported values [31]. It means that the adopted computational method and the corresponding parameters ensure us to suitably describe the phosphorene-based heterostructures in the following calculations.

Here, a phosphorene-based heterojunction is modeled by a supercell, in which a (5×1) unit cell of black-P layer is covered on a ($4\sqrt{3}$×1) unit cell of bule-P layer, as shown in FIG. 1(c). The mismatch of lattice constants between the black-P and blue-P layers is very small, namely, in the direction of x and y axes the mismatch is about 0.64% and 1.11%, respectively. The optimized vertical distance of two different monolayers is predicted to be 3.11 Å. This relative large value implies that this system is a typical vdW heterojunction. The interaction between the black-P and blue-P layers is weak, and the covalent bonding do not form at the hybrid interface.

To describe the interaction between the black-P and blue-P layers more clearly, the calculated band structures are shown in FIG. 2(a). It is clear that the proposed vdW heterojunction exhibits a direct semiconductor characteristic because the conduction band minimum (CBM) and valence band maximum (VBM) locate at Γ point. The band gap is predicted to be about 1.45 eV for the heterojunction, which is less than that of the free black-P and blue-P monolayers. This reduced band gap enables the vdW heterojunction can harvest broad spectrum of sunlight to excite more electrons from the VBs to CBs. FIG. 2(b) shows the calculated total and partial density of states (DOS). Clearly, the $3p_z$ orbitals of the black-P layer give mainly the contribution to the VBM of the proposed vdW heterojunction, while the CBM mainly originates from these 3s, $3p_x$, $3p_y$, and $3p_z$ orbitals of the blue-P layer.

According to these obtained electronic structures, as shown in FIG. 2, the proposed vdW heterojunction displays a typical type-II band alignment feature as expected. The VBM of the black-P layer is 0.37 eV higher than that of the blue-P layer, whereas the CBM of the blue-P layer is 0.13 eV lower than that of the black-P layer. This is to say, the VB and CB offsets of the black-P and blue-P monolayers are about 0.37 and 0.13 eV, respectively. This is the first prediction to explore the photoactivity of the proposed vdW heterojunction, which will be discussed in more details in below context.

To characterize the charge transfer process in the proposed vdW heterojunction, we calculate the charge density difference, which is obtained by subtracting the charge density of the vdW heterojunction from that of the free black-P and blue-P layers, and plot them in FIG. 3(a). Here, the red and blue regions stand for the accumulation and depletion of charge, respectively.

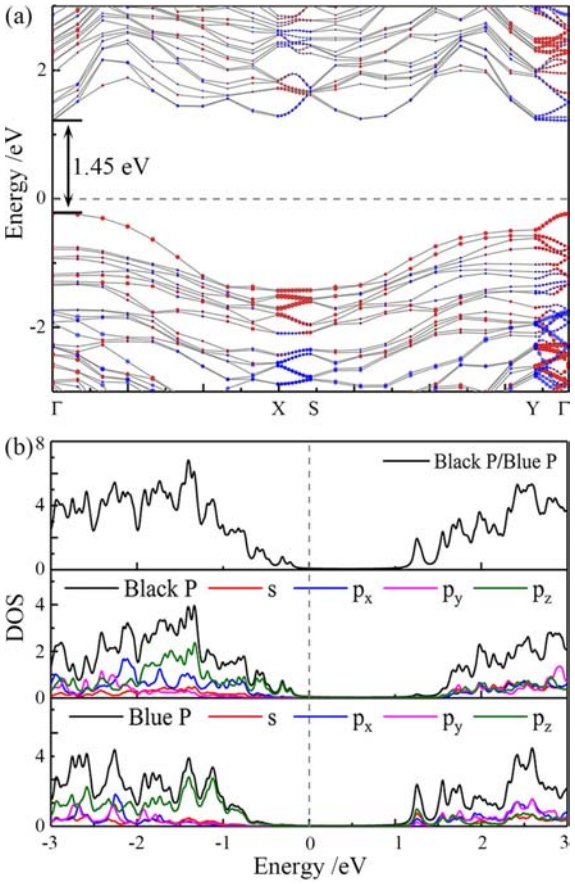

FIG. 2 (a) Calculated band structures, and (b) total and partial density of states of the vdW black-P/blue-P heterojunction at the hybrid functional HSE06 level. Here, the red and blue dots stand for the contribution from the black-P and blue-P layers, respectively, while the vertical black dashed line denotes the Fermi level.

It is clear that the charge redistribution occurs at the interface region between the black-P and blue-P layers. The holes slightly accumulate close to the blue-P layer, while the electrons accumulate close to the black-P layer. To illustrate the charge transfer more clearly, FIG. 3(b) shows the z-direction planar-averaged charge density difference, in which the positive and negative values represent electron accumulation and depletion, respectively. Again, the charge density rearranges around the interface region. Using the Bader method, further charge analysis shows that only about 0.04 e transfer from the blue-P to black-P layer. This observed interfacial charge transfer results in a built-in interfacial electric field, which can enhance the photogenerated electron-hole separation.

Based on the above presented band structures and DOS results of the proposed vdW heterojunction, the band edge alignment is illustrated in FIG. 4. Clearly, this hybrid system is a type-II heterojunction. The positions of CB and VB of the black-P layer are more positive than those of the blue-P layer. When the sunlight

DOI:10.1063/1674-0068/cjcp1811244

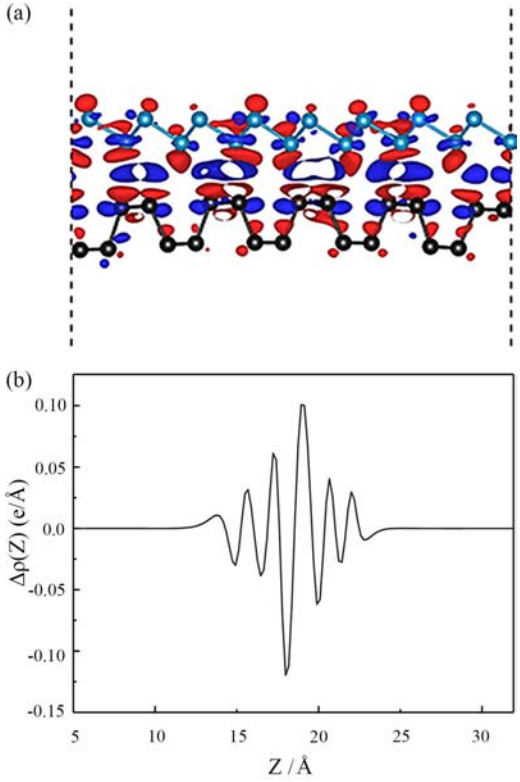

FIG. 3 (a) Charge density difference in the examined vdW heterojunction with an isosurface value of 0.00022 e/Å^3. Here, the blue and red areas represent electron depletion and accumulation, respectively. (b) The z-direction planar averaged charge density difference of the vdW heterojunction.

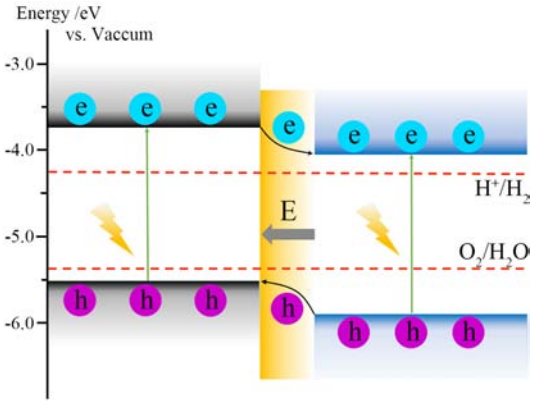

FIG. 4 Band edge alignment of the phosphorene-based vdW heterojunction. Here, the dashed red lines stand for the redoxs potentials of water.

sheds on the proposed vdW heterojunction, the electrons can be photoexcited from the CBs of both of the black-P and blue-P layers. Usually, these photoexcited electrons in the CB tend to return to the VB, and the photoexcited carriers recombine, which is extremely unfavorable to the photocatalytic reactions. Fortunately, due to the predicted typical type-II band edge match,

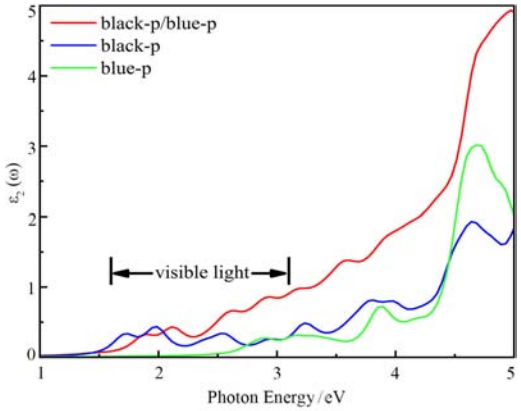

FIG. 5 Optical absorption spectra of the free black-P layer, blue-P layers, and the examined black-P/blue-P vdW heterojunction.

the photogenerated carriers (electrons) move from the CB of the black-P layer to the CB of the blue-P layer, while the photogenerated carriers (holes) transfer from the VB of the blue-P layer to the VB of the black-P layer. Then the blue-P and black-P layers provide the corresponding chemical potentials for the electrons and holes to produce hydrogen and oxygen in solar water splitting, respectively. In other words, the oxidation and reduction reactions could occur on the black-P and blue-P layers.

It should be pointed out that the polarized field (pointing from the blue-P to black-P layer) between two phosphorene layers in the vdW heterojunction further promotes the photoexcited electrons and holes accumulating on the blue-P and black-P layers, respectively. This observation is similar to the g-C_3N_4/SnS_2 heterostructure [39], but totally different from the built-in interface polarized field in the g-C_3N_4 in nanocomposite [40]. In other words, the combination of the interfacial polarized field and the type-II band alignment is helpful for the electron-hole separation. Then, the e^--h^+ recombination is greatly reduced.

In general, the optical absorption property, one of the determination indices for describing the photocatalytic performance of a semiconductor photocatalyst, is always related to its electronic structure. According to the relation: $\varepsilon(\omega)=\varepsilon_1(\omega)+i\varepsilon_2(\omega)$, one can convert the complex dielectric function to the absorption coefficient $\alpha_{\rm abs}$, then obtain the optical absorption spectra. In our calculations, by summing over a large number of empty states, the imaginary part of $\varepsilon_2(\omega)$ is chosen to represent the optical absorption efficiency. The optical absorption curves of the examined vdW heterojunction and the free black-P and blue-P layers are calculated, and plotted in FIG. 5 with the black, red, and blue lines, respectively. It is clear that, compared with the free black-P and blue-P layers, the proposed hybrid vdW heterojunction harvests more ultraviolet light, and the low-energy visible light response is significantly enhanced. This en-

DOI:10.1063/1674-0068/cjcp1811244

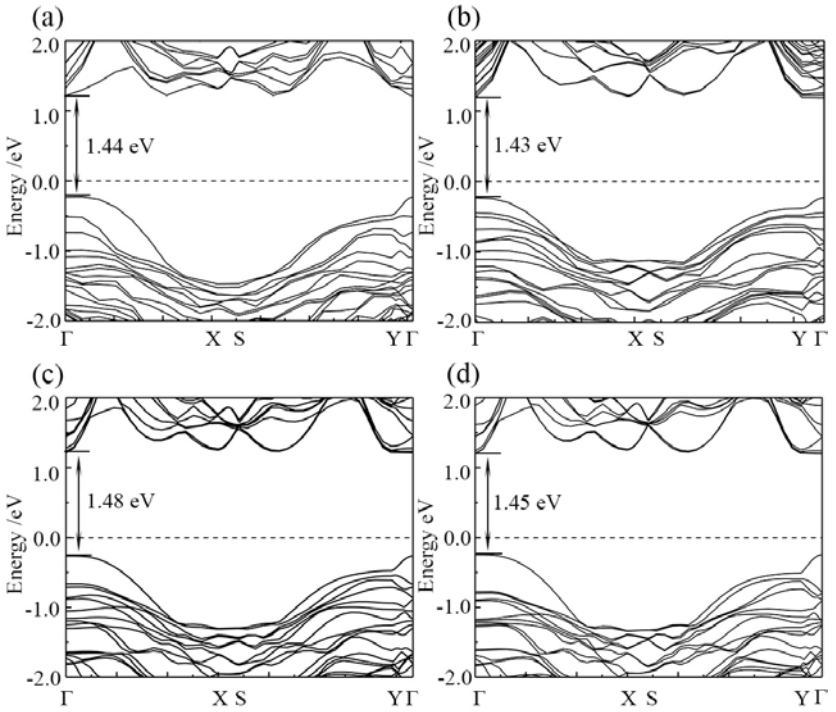

FIG. 6 Band structures of the phosphorene-based vdW heterojunction with the biaxial strain of (a) −4.0%, (b) +4.0%, and the vertical strain of (c) −4.0%, (d) +4.0%.

hancement of the optical absorption is expected to be caused by the interlayer coupling between the black-P and blue-P layers.

Note that the electronic structures and optical properties of 2D materials can be effectively modulated through introducing strain [41−43]. In experiments, the tensile or compressive strain has been demonstrated to be feasible by various strategies including external load, bending, and lattice mismatch [44]. Here, to explore the strain effect, we calculate the band structures of the proposed vdW heterojunction under the biaxial and vertical strain of −4.0% and +4.0%, respectively, and plot them in FIG. 6. The strain is simulated by changing the lattice constant, which is defined by the equation of $\varepsilon=[(a-a_0)/a_0]\times100\%$, where a and a_0 represent the lattice constants with and without strains, respectively. As shown in the FIG. 6, the direct band gaps of the vdW heterojunction just changed slightly with the applied biaxial and vertical strains, and the band gaps are predicted to be 1.44 and 1.43 eV for the biaxial strain of −4.0% and +4.0%, while they are 1.48 and 1.45 eV for the vertical strain of −4.0% and +4.0%, respectively. It indicates that the band structures of the vdW heterojunction are not sensitive to the external strain, which is highly desirable for designing photocatalyst in future experiments.

IV. CONCLUSION

In summary, we propose a phosphorene-based vdW heterojunction. Based on extensive DFT calculations at the hybrid HSE06 functional level, theoretical results including the band structures, density of states, Bader charge, and charge density difference clearly reveal that the heterojunction can effectively harvest visible light, and also have the desired VBM and CBM band edge positions to form a type-II band alignment. The photogenerated carriers can be effectively separated since the electrons and holes accumulate on the black-P and blue-P layers, respectively. On the other hand, the built-in interfacial electric field restrains the electron-hole recombination, and then enhances the photocatalytic efficiency. Moreover, we find that the band structure of the proposed vdW heterojunction is almost inert to the applied biaxial and vertical strains. These theoretical findings suggest that this phosphorene-based vdW heterojunction is a metal-free efficient photocatalyst for water splitting.

V. ACKNOWLEDGMENTS

This work was supported by the National Natural Science Foundation of China (No.21473168 and No.21873088) and the Natural Science Foundation of the Anhui Higher Education Institutions (No.KJ2016A144). Computational resources have been provided by CAS, Shanghai and USTC Supercomputer Centers.

DOI:10.1063/1674-0068/cjcp1811244

[1] Z. Zou, J. Ye, K. Sayama, and H. Arakawa, Nature **414**, 625 (2001).
[2] X. B. Chen, S. H. Shen, L. J. Guo, and S. S. Mao, Chem. Rev. **110**, 6503 (2010).
[3] Q. Li, H. Meng, P. Zhou, Y. Q. Zheng, J. Wang, J. G. Yu, and J. R. Gong, ACS Catal. **3**, 882 (2013).
[4] T. Hisatomi, J. Kubota, and K. Domen, Chem. Soc. Rev. **43**, 7520 (2014).
[5] Q. Xiang, B. Cheng, and J. Yu, Angew. Chem. Int. Ed. **54**, 11350 (2015).
[6] W. Shockley and H. J. Queisser, Appl. Phys. **32**, 510 (1961).
[7] Y. Gai, J. Li, S. S. Li, J. B. Xia, and S. H. Wei, Phys. Rev. Lett. **102**, 036402 (2009).
[8] B. Modak and S. K. Ghosh, J. Phys. Chem. C **120**, 6920 (2016).
[9] Y. Sun, H. Cheng, S. Gao, Z. Sun, Q. Liu, F. Lei, T. Yao, J. He, S. Wei. and Y. Xie, Angew. Chem. Int. Ed. **51**, 8727 (2012).
[10] R. Banerjee, R. Jayakrishnan, and P. Ayyub, J. Phys.: Condens. Matter **12**, 10647 (2000).
[11] D. Golberg, Y. Bando, Y. Huang, T. Terao, M. Mitome, C. C. Tang, and C. Y. Zhi, ACS Nano **4**, 2979 (2010).
[12] Y. Lin and J. W. Connell, Nanoscale **4**, 6908 (2012).
[13] X.Wang, K. Maeda, A. Thomas, K. Takanabe, G. Xin, J. M. Carlsson, K. Domen, and M. Antonietti, Nat. Mater. **8**, 76 (2009).
[14] J.Mahmood, E. K. Lee, M. Jung, D. Shin, I. Y. Jeon, S. M. Jung, H. J. Shin, H. J. Choi, J. M. Seo, S. Y. Seo, S. Y. Bae, S. D. Sohn, N. Park, J. H. Oh, and J. B. Baek, Nat. Commun. **6**, 6486 (2015).
[15] K. Srinivasu, B. Modak, and S. K. Ghosh, J. Phys. Chem. C **118**, 26479 (2014).
[16] C. Ataca, H. Sahin, and S. Ciraci, J. Phys. Chem. C **116**, 8983 (2012).
[17] Q. H. Wang, K. K. Zadeh, A. Kis, J. N. Coleman, and M. S. Strano, Nat. Nanotechnol. **7**, 699 (2012).
[18] M. Chhowalla, H. S. Shin, G. Eda, L. J. Li, K. P. Loh, and H. Zhang, Nat. Chem. **5**, 263 (2013).
[19] H. Liu, A. T. Neal, Z. Zhu, Z. Luo, X. F. Xu, D. Tomanek, and P. D. Ye, ACS Nano **8**, 4033 (2014).
[20] L. Li, Y. Yu, G. J. Ye, Q. Ge, X. Ou, H. Wu, D. Feng, X. H. Chen, and Y. Zhang, Nat. Nanotechnol. **9**, 372 (2014).
[21] S. Das, W. Zhang, M. Demarteau, A. Hoffmann, M. Dubey, and A. Roelofs, Nano Lett. **14**, 5733 (2014).
[22] X. Zhang, H. Xie, Z. Liu, C. Tan, Z. Luo, H. Li, J. Lin, L. Sun, W. Chen, Z. Xu, L. Xie, W. Huang, and H. Zhang, Angew. Chem. Int. Ed. **54**, 3653 (2015).
[23] L. Kou, C. Chen, and S. C. Smith, J. Phys. Chem. Lett. **6**, 2794 (2015).
[24] J. Qiao, X. Kong, Z. X. Hu, F. Yang, and W. Ji, Nat. Commun. **5**, 4475 (2014).
[25] M. Z. Rahman, C. W. Kwong, K. Davey, and S. Z. Qiao, Energy Environ. Sci. **9**, 709 (2016).
[26] B. Sa, Y. L. Li, J. Qi, R. Ahuja, and Z. Sun, J. Phys. Chem. C **118**, 26560 (2014).
[27] W. Hu, L. Lin, R. Zhang, C. Yang, and J. Yang, J. Am. Chem. Soc. **139**, 15429 (2017).
[28] H. Uk Lee, S. C. Lee, J. H. Won, B. C. Son, S. Choi, Y. Kim, S. Y. Park, H. S. Kim, Y. C. Lee, and J. Lee, Sci. Rep. **5**, 8691 (2015).
[29] L. Zhou, J. Zhang, Z. Zhuo, L. Kou, W. Ma, B. Shao, A. Du, S. Meng, and T. Frauenheim, J. Phys. Chem. Lett. **7**, 1880 (2016).
[30] H. Guo, N. Lu, J. Dai, X. Wu, and X. C. Zeng, J. Phys. Chem. C **118**, 14051 (2014).
[31] Z. Zhu and D. Tomanek, Phys. Rev. Lett. **112**, 176802 (2014).
[32] J. L. Zhang, S. Zhao, C. Han, Z. Wang, S. Zhong, S. Sun, R. Guo, X. Zhou, C. D. Gu, K. D. Yuan, Z. Li, and W. Chen, Nano Lett. **16**, 4903 (2016).
[33] P. E. Blöchl, Phys. Rev. B **50**, 17953 (1994).
[34] G. Kresse and D. Joubert, Phys. Rev. B **59**, 1758 (1999).
[35] G. Kresse and J. Hafner, Phys. Rev. B **47**, 558 (1993).
[36] J. P. Perdew, K. Burke, and M. Ernzerhof, Phys. Rev. Lett. **77**, 3865 (1996).
[37] S. Grimme, Comput. Chem. **27**, 1787 (2006).
[38] G. Henkelman, B. P. Uberuaga, and H. Jónsson, J. Chem. Phys. **113**, 9901 (2000).
[39] S. H. Chen, J. J. Wang, J. Huang, and Q. X. Li, Chin. J. Chem. Phys. **30**, 36 (2017).
[40] J. J. Wang, Z. Y. Guan, J. Huang, Q. X. Li, and J. L. Yang, J. Mater. Chem. A **2**, 7960 (2014).
[41] Y. Chen, Q. Sun, and P. Jena, J. Mater. Chem. C **4**, 6353 (2016).
[42] X. Qian, L. Fu, and J. Li, Nano Res. **8**, 967 (2015).
[43] D. D. Wang, D. X. Han, L. Liu, and L. Niu, RSC Adv. **6**, 28484 (2016).
[44] Y. L. Jiao, L. J. Zhou, F. X. Ma, G. P. Gao, L. Z. Kou, J. Bell, S. Sanvito, and A. J. Du, ACS Appl. Mater. Interfaces **8**, 5385 (2016).

DOI:10.1063/1674-0068/cjcp1811244